HHS Public Access

Author manuscript

Bone. Author manuscript; available in PMC 2022 June 01.

Published in final edited form as:

Bone. 2021 June ; 147: 115906. doi:10.1016/j.bone.2021.115906.

Type 1 diabetic Akita mice have low bone mass and impaired fracture healing

Pei Hu[a,b], **Jennifer A. McKenzie**[b], **Evan G. Buettmann**[b,c], **Nicole Migotsky**[b,c], **Michael J. Gardner**[d], **Matthew J. Silva**[b,c,*]

[a]State Key Laboratory of Oral Diseases, West China School of Stomatology, Sichuan University, Chengdu, 610041, Sichuan, China

[b]Department of Orthopaedic Surgery and Musculoskeletal Research Center, Washington University School of Medicine, Saint Louis, MO, United States

[c]Department of Biomedical Engineering, Washington University, Saint Louis, MO, United States

[d]Department of Orthopaedic Surgery, Stanford University School of Medicine, Stanford, CA, United States

Abstract

Type 1 diabetes (T1DM) impairs bone formation and fracture healing in humans. Akita mice carry a mutation in one allele of the insulin-2 (*Ins2*) gene, which leads to pancreatic beta cell dysfunction and hyperglycemia by 5–6 weeks age. We hypothesized that T1DM in Akita mice is associated with decreased bone mass, weaker bones, and impaired fracture healing. Ins2 +/− (Akita) and wildtype (WT) males were subjected to femur fracture at 18-weeks age and healing assessed 3–21 days post-fracture. Non-fractured left femurs were assessed for morphology (microCT) and strength (bending or torsion) at 19–21 weeks age. Fractured right femurs were assessed for callus mechanics (torsion), morphology and composition (microCT and histology) and gene expression (qPCR). Both Akita and WT mice gained weight from 3 to 18 weeks age, but Akita mice weighed less starting at 5 weeks (−5.2%, $p < 0.05$). At 18–20 weeks age Akita mice had reduced serum osteocalcin (−30%), cortical bone area (−16%), and thickness (−17%) compared to WT, as well as reduced cancellous BV/TV (−39%), trabecular thickness (−23%) and vBMD (−31%). Mechanical testing of non-fractured femurs showed decreased structural (stiffness, ultimate load) and material (ultimate stress) properties of Akita bones. At 14 and 21 days post fracture Akita mice had a significantly smaller callus than WT mice (~30%), with less cartilage and bone area. Assessment of torsional strength showed a weaker callus in Akita mice with lower stiffness (−42%), maximum torque (−44%) and work to fracture (−44%). In summary, cortical and cancellous bone mass were reduced in Akita mice, with lower bone mechanical properties. Fracture healing in Akita mice was impaired by T1DM, with a smaller, weaker fracture callus due to decreased cartilage and bone formation. In conclusion, the Akita mouse mimics some of the skeletal features of T1DM in humans, including osteopenia and impaired fracture healing, and may be useful to test interventions.

*Corresponding author: silvam@wustl.edu.

Keywords

Akita diabetic mouse; Bone strength; Fracture healing; Bone formation; Cartilage

1. Introduction

Diabetes mellitus (DM) is a group of metabolic diseases affecting an estimated 400 million people worldwide, characterized by high blood sugar which can cause severe complications including cardiovascular disease, stroke and chronic kidney disease (25, 44). Type 1 diabetes (T1DM) manifests in children and young adults, with 80,000 new cases in the U.S. each year (5). T1DM is marked by insulin deficiency due to loss of the insulin-producing beta cells of the pancreatic islets, due in most cases to T cell-mediated autoimmune attack (7, 42). T1DM is associated with low bone mass via suppressed bone formation in human patients (15, 30, 33). Moreover, fracture risk is increased and fracture healing is impaired in human T1DM patients (14, 17, 18, 48, 52). The mechanisms underlying osteopenia and poor fracture healing in T1DM are not fully understood, and both pharmacologic and genetically predisposed rodent models are needed to study this issue.

T1DM is commonly induced in rodents by exposure to the toxin streptozotocin (STZ) (41), which is well documented to cause osteopenia and reduced bone strength (3, 34, 45) as well as impaired fracture healing (2, 20, 26, 28). Advantages of this approach include temporal control and applicability to many strains of mice and rats. On the other hand, limitations for bone studies include its dose-dependent skeletal phenotype, and concomitant weight loss and altered body composition which can secondarily affect the skeleton (3, 32, 45). Moreover, streptozotocin is toxic to not only beta cells, but all cells expressing the glucose transport protein GLUT2, which makes it challenging to isolate the effects of diabetes (50).

The Akita mouse is an alternative T1DM model that has a mutation in the *Ins2* gene, one of two genes that encodes insulin in mice (49, 53). Akita mice are born with normal pancreatic islets and insulin-producing β cells, but the *Ins2* mutation leads to accumulation of misfolded proinsulin protein, pancreatic beta cell dysfunction and apoptosis, and hypoinsulinemia (37, 39, 49). Near 5-weeks of age, male Akita mice become spontaneously diabetic with high blood glucose but without obesity or insulitis; diabetic presentation in female Akita mice is less severe and more variable (24). Compared to STZ-induced mice, male Akita mice are similarly hyperglycemic but with less severe loss of body weight and sarcopenia (6). Akita mice also appear to have a milder osteopenia than STZ mice, although there are conflicting reports on the severity of the phenotype in cortical and cancellous bone, perhaps related to mouse age (adolescent vs. adult) (4, 6). Importantly, it is not known if male Akita mice have reduced bone mechanical properties or impaired fracture healing as seen in STZ-induced rodents and in human patients. Addressing these knowledge gaps may strengthen the rationale for use of Akita mice to model T1DM effects on the skeleton.

Our goals were 1) to further evaluate the skeletal phenotype of male Akita mice including bone mechanical properties, and 2) to assess whether Akita mice have altered fracture healing compared to wildtype controls. We focused on young-adult male mice, aged 18–21 weeks, which allowed for cumulative T1DM effects during the period of rapid skeletal

growth, and corresponds with the age when Akita males reach peak body weight (53). We found that T1DM in Akita mice is associated with decreased bone mass and mechanical properties, and impaired fracture healing. These findings support the use of Akita mice for studies of the skeletal complications of diabetes.

2. Methods

2.1 Mice

All protocols and experiments described were approved by the Washington University IACUC. Male heterozygous C57BL/6-*Ins2*^{Akita}/J mice (Akita, stock No. 003548) and female C57Bl/6J mice (wildtype, stock No. 000664) purchased from Jackson Laboratory were set up as breeders at 8-weeks age. Mice were genotyped using qPCR (Transnetyx, Ins2-1 MUT probe). Experimental mice were littermate males heterozygous for the mutation (Ins2-1 MUT probe present, Akita) and males without the mutation (wildtype, WT). Akita and WT mice were housed together under standard conditions. A total of 167 mice were used (69 Akita, 98 WT), with serum glucose measured on all mice. Unilateral (right) femur fractures were created at 18 weeks, and mice were euthanized 3 to 21 days later. Bilateral femora were harvested at post-fracture days 3 (D3, n = 13 Akita, n = 16 WT), 7 (D7, n = 14 Akita, n = 18 WT), 14 (D14, n = 15 Akita, n = 24 WT) and 21 (D21, n = 20 Akita, n= 29 WT), with euthanasia performed by CO_2 asphyxiation (except where otherwise noted). Group sample sizes are indicated for each outcome below. A subset of Akita and WT mice were not fractured (Non-Fx; n = 6/group) and used for baseline serum measurements at 18 weeks. All other data presented are from mice subjected to fracture.

2.2 Body weight, glucose and serum measurements

Body weight was recorded weekly from 3 to 18 weeks age (n=28–40/group). At 6 and 18 weeks, a 6-hour fasting blood glucose level was tested using a drop of tail vein blood (Arkray Glucocard, range 0–600 mg/dL). Blood glucose levels greater than 250 mg/dL were defined as diabetic. Serum from the Non-Fx group, and from a subset of days 3, 7, 14 and 21 post-fracture groups (n=6/group) was analyzed for insulin (Singulex), osteocalcin (OCN; Immutopics mouse osteocalcin ELISA kit) and CTX-1 (ids RatLaps™ CTX-I EIA kit). To obtain serum, mice were fasted for 6 hours then sedated using 1–3% isoflurane. A terminal blood collection was performed from the orbital sinus and the mouse was euthanized by cervical dislocation. Blood was set at room temperature for 1 hour to clot and then centrifuged 13,000 rpm at 4°C for 6 min in blood collection tubes (BD Biosciences). Upper serum was collected and kept at −80°C until submission to Core Laboratory for Clinical Studies (Washington University).

2.3 Bone phenotyping and mechanical testing on intact femurs

Intact (left, non-fractured) femurs were harvested at 21 weeks age (post fracture day 21) from Akita and WT mice for cortical bone analysis and three-point bending tests (n = 10/group), and at 19 weeks age (post fracture D7) for cancellous bone analysis (n = 7/group). Bones were wrapped in saline-soaked gauze and stored frozen at −20°C until use. Femur lengths were measured with a digital caliper; femurs were then scanned by microCT (vivaCT 40, Scanco Medical AG, 10.5 μm, 1000 projections, 300 ms, 70 kVp,

114 μA, high resolution) and analyzed using the Scano software. For cortical analysis, the region of interest (ROI) was defined as 1.05 mm (100 slices) in the mid-diaphysis. Contours were drawn on the periosteal surface of the bone (analysis parameters: sigma 0.4, support 1, threshold 350 mg HA/cm^3). Cortical analysis parameters included total area (Tt.Ar), bone area (Ct.Ar), bone area fraction (Ct.Ar/Tt.Ar), medullary area (Ma.Ar), cortical bone thickness (Ct.Th), polar moment of inertia (pMOI), minimum moment of inertia (Imin), maximum moment of inertia (Imax) and tissue mineral density (TMD). For cancellous analysis the ROI was defined as 2.10 mm (200 slices) proximal to the distal (knee) growth plate. Contours were drawn on the endosteal surface of the cortical bone (analysis parameters: sigma 0.4, support 1, threshold 220 mg HA/cm^3). Cancellous analysis parameters included total volume (TV), bone volume (BV), bone volume fraction (BV/TV), connectivity density (Conn-Dens), structure model index (TRI-SMI), trabecular number (Tb.N), trabecular thickness (Tb.Th), trabecular separation (Tb.Sp), and volumetric bone mineral density (vBMD). After microCT and following one freeze/thaw cycle, the left femurs used for cortical analysis were subjected to three-point bending according to published guidelines (19) (span = 7 mm, monotonic ramp, 0.1 mm/s; Dynamight 8841, Instron). Force-displacement plots were analyzed to determine structural properties: stiffness, yield load, maximum (ultimate) load, post-yield displacement, and work to fracture. Material properties were estimated using simple beam theory (19): yield stress, ultimate stress, and Young's modulus.

2.4 Femur fracture

Right femur mid-point full fracture was performed when mice were 18-weeks old as previously described (27). Mice were given buprenorphine SR (1 mg/kg, s.c.) 1 hour before surgery and sedated (1–3% isoflurane) during surgery. Briefly, the mid-femur was exposed and notched with a #12 blade to predispose the site to fracture. A transverse fracture was made using position-controlled loading (Dynamight 8841, Instron; 30 mm/s in the posterior direction), applied to the anterior mid-diaphysis and stabilized with a 24-gauge pin. Radiographs were taken both after surgery and before euthanasia to confirm pin placement (3X magnification; Faxitron UltraFocus100). Endpoint lateral radiographs were scored for callus bridging. Using a modified Goldberg scale radiographs were blindly scored for the degree of healing (0 = no bridging, 1 = one side bridged, 2 = complete bridging) (13). One mouse was excluded from the study to do a missing pin at euthanasia. After anesthesia recovery, mice were returned to their cages without activity restrictions. Sutures were checked daily for 3 days and removed at day 7.

2.5 Right femur callus microCT analysis

Right femurs from days 14 and 21 after fracture were scanned with pins removed using microCT (n=7–10/group/time) (VivaCT 40, Scanco Medical AG, 21 μm voxel size, 1000 projections, 300 ms, 55 kVp, 145 μA, high resolution). Callus analysis was done using the manufacturer's cancellous analysis tools on a 6.3 mm (300 slice) ROI centered at the midpoint of the fracture. Contours were drawn on the outer surface of the callus (analysis parameters: sigma 0, support 0, threshold 150 mg HA/cm^3). Total volume (TV), bone volume (BV), bone volume fraction (BV/TV) and volumetric bone mineral density (vBMD) were analyzed. Femurs were used for histology analysis after scanning.

2.6 Mechanical strength testing using torsion

Intact left and fractured right femurs from day 21 post fracture Akita and WT mice were subjected to torsion testing to assess strength recovery (n=9–13/group). Both femur ends were potted in acrylic tubes (6 mm diameter × 12 mm length) with polymethylmethacrylate (Ortho-Jet, Lang Dental), leaving the middle 7 mm diaphyseal region as the gage region. Samples were soaked with phosphate buffered saline before testing. A custom-built torsion tester with a 25 in-oz load cell and Labview (Labview 2014) was used for testing and data collection. With one end fixed, the opposite end was rotated from 0 to 360 degrees at 1 deg/s. Torque-rotation plots were analyzed for stiffness, maximum torque, rotation at maximum torque, torque at fracture, rotation at fracture, and work to fracture.

2.7 Right femur callus histology

Femurs with surrounding soft tissue from days 7, 14 and 21 after fracture were fixed for 24 hours in 10% neutral buffered formalin and decalcified for 2 weeks with 14% EDTA (n = 7–11/group/timepoint). The femurs were embedded in paraffin, longitudinally sectioned at 5 μm and serial sections were stained with hematoxylin and eosin (H&E), picrosirius red/alcian blue, tartrate-resistant acid phosphatase (TRAP) or endomucin. The stained slides were imaged (Hamamatsu Nanozoomer HT) at 20x magnification across the entire femur. Picrosirius red/alcian blue stained images were quantified for callus area (excluding cortical bone and marrow), and areas of the three callus tissues: woven bone area, cartilage area and fibrous tissue area. In woven bone regions, TRAP stained images were quantified for osteoclast number (Oc.N), osteoclast surface (Oc.S) and woven bone surface (Bioquant v18, Nashville, TN). On a single section per femur, two to four representative 20x regions were analyzed and averaged for each mouse by a blinded observer. The vasculature was visualized using immunohistochemistry for endomucin on paraffin sections (rat monoclonal eBioV.7C7, ebisocience; 1:400 dilution). Sections were deparaffinized in xylene and rehydrated in graded ethanol. Antigen retrieval was done using proteinase K (5 min, room temp) and the Vectastain Elite ABC HRP kit (Vector Labs; PK-6104). Negative controls were run with an isotype antibody (Clone eBR2a, ebioscience; 1:400 dilution). ImmPact DAB Peroxidase (HRP) Substrate kit was used for detection (Vector Labs; SK-4105). Analysis of endomucin stained images was performed on the woven bone regions of the callus, to quantify vessel number, vessel density, percent vessel area, and percent mineralized area on two to four representative 20x regions per section, similar to TRAP analysis.

2.8 Gene expression

On days 3, 7 and 21 after fracture, the central 8 mm of fractured right femurs (including callus and cortical bone) and non-fractured left femurs (cortical bone only) were dissected free of adjacent tissues (n=3–6/group/timepoint). The marrow was removed by centrifugation and the samples were frozen in liquid nitrogen. Total RNA was extracted using RNeasy Mini kit (Qiagen) after samples were pulverized with Mikro-Dismembrator U (B. Braun Biotech International) and stabilized with Trizol (Ambion). RNA concentration was quantified (Nanodrop ONE, Thermal Scientific) and RNA integrity numbers (RIN) evaluated (Bioanalyzer 2100, Agilent Technologies). Only RNA with

260/280 nm absorbance ratio of 1.8–2.1 and RIN ≥ 7 were used. cDNA was produced (iScript, Biorad) from 250 ng of total RNA and qRT-PCR was performed by the Genome Technology Access Center (GTAC, Washington University in St. Louis) using TaqMan probes and 96 × 96 high-throughput chips on BioMark HD System. A total of 23 genes were evaluated in triplicate: 2 reference genes – TATA box binding protein (*Tbp*) and importin 8 (*Ipo8*); 4 osteogenic genes – collagen type I alpha 1 chain (*Col1a1*), bone gamma-carboxyglutamic acid-containing protein (*Bglap*), runt related transcription factor 2 (*Runx2*) and sclerostin (*Sost*); 3 chondrogenic genes – aggrecan (*Acan*), SRY (sex determining region Y)-box 9 (*Sox9*) and collagen type II alpha 1 chain (*Col2a1*); 3 Hedgehog pathway mediators – Indian Hedgehog (*Ihh*), patched 1 (*Ptch1*) and GLI Family Zinc Finger 1 (*Gli1*); 1 osteoclastogenic gene – cathepsin K (*Ctsk*); 4 inflammatory genes – tumor necrosis factor (*Tnf*), interleukin 6 (*Il6*), prostaglandin-endoperoxide synthase 2 (*Ptgs2*) and colony stimulating factor 1 (*Csf1*); and 4 angiogenic genes – vascular endothelial growth factor A (*Vegfa*), angiopoietin 2 (*Angpt2*), nitric oxide synthase 2 (*Nos2*) and hypoxia inducible factor 1 subunit alpha (*Hif1a*). Expression was calculated for each sample relative to the reference genes ($2^{-\Delta CT}$), and also calculated as fold-change of fractured vs. paired intact ($2^{-\Delta\Delta CT}$).

2.9 Statistical analysis

Group sample sizes (n) for primary fracture healing outcomes were chosen based on *a priori* sample size calculation. Using prior data to estimate variance (31), and an effect size of 30% for callus bone volume, and 40% for callus stiffness, a minimum sample size of n=8 was indicated (alpha [significance] = 0.05, and beta [type II error] = 0.2). Data are presented as means and standard deviation. All data sets were tested for normality. If data were normally distributed, an unpaired t-test was used to compare between WT and Akita groups; if not, a nonparametric Mann-Whitney test was used for comparisons. 2-way ANOVA with Sidak test were used to analyze changes between groups over time. Because there was a body weight difference between genotypes, any variable that was not already size-adjusted was regressed against body weight, for each group (genotype) separately. Using a linear regression model (19) many variables were not significant correlated with body weight and adjustments were not made to the data. If outcomes were significant correlated with body weight we also computed body-weight adjusted values using linear regression and re-ran the statistics. The adjusted data are presented in supplemental materials. All tests were done using PRISM (GraphPad PRISM Software). Statistical significance was considered at $p<0.05$, and trends were noted at $p<0.10$.

3. Results

3.1 Akita mice have early onset, severe hyperglycemia

To confirm T1DM in male Akita mice, body weight, fasting blood glucose and serum insulin levels were assessed. Both Akita and WT mice gained weight from 3 to 18 weeks of age (Figure 1A). However, at 6 weeks, Akita mice began to weigh less than their WT litter mates (−6.5%, p=0.015) and the difference increased slightly as mice matured to 18 weeks (−9.2%, $p<0.001$). All Akita mice were hyperglycemic by 6 weeks (average: 496 mg/dL), which became more severe at 18 weeks (average: 574 mg/dL) (Figure 1B). We observed polyuria,

polydipsia and polyphagia in Akita mice, with increased food and water consumption (not shown). Analysis of serum insulin at 18 weeks confirmed that Akita mice were severely insulin deficient (Figure 1C, −93%, p=0.016). Thus, male Akita mice develop T1DM by 6 weeks age but continue to gain body weight.

3.2 Akita mice have modestly reduced cortical and cancellous bone mass

We assessed the skeletal phenotype of Akita and WT mice using microCT of intact femora (Figure 2, Suppl. Table S1). Akita mice had a slightly shorter (−1.9%) femur than WT (Figure 2B, p<0.001) and reduced measures of cortical and cancellous bone mass. Specifically, the cortical diaphysis of Akita femurs had reduced total area (−6.5%, p<0.05, Figure 2C), bone area (−16%, p<0.001, Figure 2D), and cortical thickness (−17%, p<0.001, Figure 2E), which resulted in a lower Ct.Ar/Tt.Ar (−9.8%, p<0.005) and polar moment of inertia (pMOI, −21%, p<0.001, Figure 2F). Medullary area (Figure 2G) and tissue mineral density (Figure 2H) were not different between groups. Similarly, the cancellous bone microCT results (Figure 2I–L, Suppl. Table S1) showed that Akita femurs had reduced bone volume (−41%, p=0.040), BV/TV (−39%, p=0.021, Figure 2K), trabecular thickness (−23%, p<0.001, Figure 2J), and volumetric bone mineral density (−31%, p=0.009, Figure 2L), with no change in total volume. Four cortical morphology parameters were significantly correlated with body weight and adjusted values were calculated based on linear regression (Suppl. Table S1). In only one case did the ANOVA analysis of adjusted values yield a different conclusion than the non-adjusted data; Tt.Ar was not significant after adjustment (−3.4%, p=0.12). Lastly, serum OCN was decreased in Akita mice (−30%, p<0.05) while serum CTX-1 was not different from control (Figure 2M–N). In summary, femurs from male Akita mice are modestly osteopenic, even after accounting for their smaller body weight, in association with low bone formation.

3.3 Akita femurs have reduced whole-bone strength but are not brittle

Three-point bending on intact femurs revealed reduced whole-bone (structural) properties in Akita femurs compared to WT (Figure 3A–F, Suppl. Table S2). Specifically, Akita femurs had decreased stiffness (−24%, p=0.002, Figure 3B), maximum load (−27%, p=0.001, Figure 3C) and yield load (−26%, p=0.036, Figure 3D). On the other hand, Akita femurs had increased post-yield displacement (62%, p=0.015, Figure 3E), with no difference in work to fracture (Figure 3F), which indicate they did not have brittle material behavior. Considering the estimated material properties, Young's modulus and yield stress were not different between groups (Figure 3G–H), while ultimate stress was decreased in Akita femurs (−16%, p=0.019, Figure 3I). None of the structural properties correlated significantly with body weight (Suppl. Table S2). Thus, femurs from Akita mice were less stiff and strong at the whole-bone level, while at the material level they showed a modest decrease in strength (ultimate stress) but no evidence of brittleness.

3.4 Akita mice have diminished callus bone formation in fracture healing

Both WT and Akita mice lost weight over the first 7 days after fracture, but then regained it; by 21 days after fracture differences in body weight between groups were not significant (Suppl. Figure S1, Suppl. Table S3). Endpoint radiographs were assessed in Akita and WT mice at days 14 and 21 (Figure 4A). Quantification of callus bridging showed that

Akita calluses had lower union rates than WT (D21 Chi-squared $p < 0.05$, Figure 4B). We performed microCT scanning of fractured femora on days 14 and 21 post fracture to assess callus size and mineralization (Figure 4C, Suppl. Table). On day 14, Akita mice had a significantly lower total volume (−29%, $p<0.001$, Figure 4D) and bone volume (−17%, $p<0.001$, Figure 4E) compared to WT, although with significantly higher BV/TV (19%, $p=0.035$, Figure 4F) and volumetric bone mineral density (vBMD, 25%, $p=0.018$, Figure 4G). On day 21, Akita calluses also had a lower total volume (−24%, $p=0.001$) and bone volume (−21%, $p<0.001$) versus WT, while BV/TV and vBMD showed no differences between groups (Figure 4C–G). Only one callus microCT parameter (D21 total volume) was correlated with body weight, and this remained significantly reduced in Akita mice after body weight adjustment (Suppl. Table S4). Thus, microCT showed that Akita mice had smaller calluses with less bone volume compared to WT, although measures of callus mineralization (i.e., BV/TV and vBMD) were not impaired in Akita mice.

We next assessed outcomes related to bone formation, both systemically (serum ELISA) and locally (callus qPCR). Compared to WT, Akita mice had lower serum OCN at days 7, 14 and 21 post-fracture (Figure 4H), indicating lower systemic bone formation, consistent with their relative osteopenia and lower callus bone volume. However, the relative expression of osteogenic genes showed no differences between groups, with the exception of lower *Runx2* expression on day 14 in fracture callus from Akita mice (Figure 4I–K). Collectively, these findings point to less absolute bone formation in Akita mice, but little impairment in osteogenesis was detected at the mRNA level.

3.5 Akita mice had impaired cartilage formation in fracture healing

To assess whether chondrogenesis was influenced in Akita fracture healing, histological sections and qPCR of callus tissue were analyzed. Based on the quantification of picrosirius red/alcian blue stained sections (Figure 5A), Akita mice had a smaller callus area at all time points (day 7: −25%, $p=0.045$; day 14: −26%, $p=0.010$; day 21: −32%, $p=0.013$), and less woven bone area on day 21 (−35%, $p=0.002$) (Figures 5B–C), both consistent with microCT results. Furthermore, Akita mice had markedly less cartilage on day 7 (−69%, $p=0.021$) and day 14 (−51%, $p<0.001$) (Figure 5D). qPCR analysis showed that the expression of chondrogenic genes (*Acan*, *Sox9* and *Col2a1*) was many fold greater in fractured compared to intact bones in both groups, especially on day 7 and day 14 (Figure 5F). The relative expression of these genes was 2–7 times lower in day 7 Akita fractured femurs compared to WT fractured femurs ($p < 0.05$; Suppl. Table S5), although these differences were not significant after normalizing to intact femurs (Figure 5F). Similar changes were observed for expression of hedgehog pathway related genes (*Ihh*, *Ptch1* and *Gli1*). Thus, calluses from Akita mice had smaller cartilage area and evidence of less robust upregulation of some chondrogenic genes after fracture.

3.6 Fracture callus in Akita mice had fewer osteoclasts at day 7

Analysis of TRAP stained sections of woven bone in the fracture callus revealed abundant osteoclasts, consistent with rapid turnover (Figure 6A–B). On day 7, Akita mice had reduced osteoclast number (Oc.N/BS, −37%) and osteoclast surface (Oc.S/BS, −43%) compared to WT mice (Figure 6C–D; Suppl. Table S6). On days 14 and 21, osteoclast measures were not

different between groups. In addition, osteoclasts appeared in similar abundance at cartilage-bone interfaces in Akita and WT callus (not shown). We also assessed serum CTX-1 levels and expression of osteoclast-related genes. CTX-1 did not differ between groups, except on day 14 when it was higher in Akita mice (Figure 6E). On the other hand, at this same time point, expression of the osteoclast marker *Ctsk* was lower in the Akita group (Figure 6F). Other genes related to osteoclastogenesis or inflammation (*Tnf*, *Il6*, *Ptgs2*, *Csf1*) were not different between groups when comparing fold-change (fractured/intact) values (Suppl. Table S5) Thus, outcomes related to bone resorption were not consistently altered in Akita mice.

3.7 Angiogenesis in fracture callus of Akita femurs is normal

The quantitative analysis of endomucin staining showed no difference between Akita and WT fracture healing both on day 7 and 14 (Suppl. Table S7). Consistent with histology results, no significance was found in gene expression of angiogenic genes *Vegfa*, *Angpt2*, *Nos2* and *Hif1a* (Suppl. Table S5).

3.8 Akita femurs have inferior fracture callus torsional stiffness and strength

To assess if recovery of bone strength after fracture is affected by T1DM, fractured and intact femurs from Akita and WT were tested in torsion at day 21, a time when callus strength is expected to approach intact levels in normal, young mice (27). Consistent with results of three-point bending, torsion tests of *intact* femora found that Akita mice had lower stiffness (−20%, $p=0.036$) and maximum torque (−22%, $p=0.001$) than WT; work to fracture was also lower in Akita femora (−25%, $p=0.036$) (Figure 7A–C, Suppl. Table S8). Tests of *fractured* bones showed that calluses from Akita mice had lower absolute stiffness (−42%, $p<0.01$), maximum torque (−44%, $p<0.05$), rotation at fracture (−36%, $p<0.05$), and work to fracture (−44%, $p<0.05$) (Figure 7D–F, Suppl. Table S8). Analysis of normalized values (fractured/intact) revealed that stiffness and maximum torque were significantly less than 1.0, indicating that functional healing had not been achieved at day 21 in either group. However, normalized stiffness of fractured Akita femurs was significantly less than WT (−28%, $p=0.043$; Figure 7G), indicating a slower rate of functional healing in Akita mice. In summary, fracture callus from Akita mice had inferior mechanical properties compared to WT, and with evidence of impaired recovery of stiffness at day 21 post fracture.

4. Discussion

Akita mice are an alternative to toxin-induced models of type 1 diabetes mellitus (T1DM), although they have not been as widely used for studies of skeletal complications. Our first goal was to evaluate the skeletal phenotype of adult male Akita mice. We observed spontaneous hyperglycemia in 100% of Akita mice by 6 weeks age, resulting in at least 12 weeks of diabetes prior to evaluation. Results of microCT and mechanical testing support our hypothesis that T1DM in male Akita mice is associated with decreased bone mass and mechanical properties. Low bone mass was observed in both cortical and cancellous bone, and is attributed to low bone formation. Our second goal was to assess fracture healing in Akita mice. We find that fracture healing is impaired in femurs of Akita mice, which have smaller callus volume and reduced torsional stiffness and strength compared to non-diabetic

control mice. These findings support the use of Akita mice for studies of the skeletal complications of diabetes.

Impaired fracture healing has been documented in human patients with diabetes (20, 48). We find that T1DM Akita mice also have impaired endochondral fracture healing at the timepoints we tested. Torsional testing of femurs 21 days after fracture demonstrated that stiffness, maximum torque and work to fracture were 40–45% lower in Akita mice than in littermate controls. The inferior mechanical properties are consistent with a smaller fracture callus, evident by microCT and histology. In absolute terms, both callus bone volume and cartilage volume are less in Akita mice. The reduced size of the bone callus is consistent with lower serum osteocalcin (i.e., lower bone formation) in Akita mice 7–21 days post-fracture. However, there was no clear osteogenic deficit detected at the level of callus mRNA expression. On the other hand, the relative expression of chondrogenic genes was significantly lower in fracture callus from Akita mice compared to control mice, consistent with reduced cartilage formation. This effect is likely related to the loss of insulin, which is an anabolic factor in chondrogenesis (11, 40, 51). Notably, we do not find evidence that the smaller bone and cartilage in Akita is explained by exuberant osteoclast number or activity, or by impaired angiogenesis. Taken together, our data suggest that the smaller fracture callus in Akita mice is due to primary defects in bone and cartilage formation.

Our finding of impaired fracture healing in male Akita mice is consistent with reports in other rodent models of diabetes, albeit with some differences. BB rats, an inbred strain that develops spontaneous T1DM, have lower callus bone and cartilage area after fracture, and lower mechanical properties compared to normoglycemic controls (8, 12), similar to our findings. These effects were reversed by systemic or local delivery of insulin (8, 12), which suggests that treatment with insulin, a known bone and cartilage anabolic factor (9, 11, 40, 47, 51), will improve healing in Akita mice.

Streptozotocin (STZ)-induced T1DM in rats and mice also results in smaller cartilage and bone fracture callus, and reduced callus mechanical properties (2, 10, 23, 28, 35). Results in STZ-induced rodents show increased osteoclast-related gene expression and osteoclasts in the callus, as well as accelerated cartilage resorption (2, 16, 21, 23, 35). In contrast, we find no difference in osteoclast-related gene expression and normal or reduced callus osteoclasts in Akita mice. Furthermore, while cartilage area is diminished (and chondrogenic genes are less upregulated), the rate of cartilage resorption appears similar in Akita and WT mice, with both decreasing from 14 to 21 days. This notable distinction between STZ and Akita models suggests that some mechanisms shown to influence impaired healing and exuberant cartilage removal in STZ mice, including TNF-alpha and FOX01 (1, 2, 22), may not be as important in Akita mice. Additional studies will be needed to test this hypothesis.

MicroCT analysis of the intact femurs of male Akita mice show mild cortical and cancellous osteopenia, even after adjusting for their modestly reduced body weight. Their low bone mass is associated with low bone formation (reduced serum OCN; Fig. 2N) rather than elevated resorption (normal CTX-1; Fig. 2M). Coe et al. (6) reported a similar phenotype in younger (10-wk old) male Akita mice, i.e., low cancellous bone mass and serum OCN, although they did not detect differences in cortical bone at this age. Notably, the deficit

in basal bone formation is consistent with a report showing reduced anabolic response to mechanical loading in male Akita mice (38). Carvalho et al. (4) recently reported low cortical bone mass in male Akita mice at 4–12 months, consistent with our findings, but surprisingly high cancellous bone mass in the distal femur, which differs from our results and Coe et al. (6) at the same site. The reason for the difference in cancellous bone outcomes between these studies is unclear. Notably, studies of STZ-induced diabetes report consistent deficits in cortical and cancellous sites (6, 29, 34, 45), as we find for Akita mice in this study.

Mechanical testing showed lower whole-bone properties in male Akita femurs, consistent with their smaller bone size. Maximum load was 27% lower in Akita mice, which corresponded with a reduction in cortical area of 16%. This slight discrepancy in altered strength-per-area explains why Akita bones had a modest reduction in estimated ultimate stress, a measure of material strength. Ohuchi et al. (36) recently reported no significant difference in whole-bone mechanical properties in 12-week old, female Akita mice, although the mice in their study had a shorter duration of T1DM and had less severe hyperglycemia than mice in our study (~400 mg/dL vs. ~500–600 mg/dL), as expected for female Akita (38). In STZ diabetic rats (45) and mice (34), both whole-bone mechanical properties and estimated material properties are lower than normal, which is consistent with our current findings. One difference is that Nyman et al. (34) reported that STZ diabetic femurs had reduced post-yield displacement, indicating brittle behavior, whereas we find the opposite in Akita femurs despite similar levels of hyperglycemia. We note that the increased post-yield displacement we observed in Akita femurs may be due in part to their more slender morphology (i.e., lower section modulus, Suppl. Table 2). Additional studies will be needed to confirm whether Akita mice are less susceptible to glycosylation-mediated bone embrittlement than other diabetic rodents (43).

Akita mice offer some pros and cons compared to the more common STZ-induced model of T1DM. Despite severe hyperglycemia by 6 weeks age, Akita mice gained weight through 18 weeks with normal care, at which time they were only 9% lighter than WT littermates. This weight difference is similar to a previous report (6), and less than the 20–25% values reported for similarly aged STZ-induced diabetic mice (3, 6, 34). Although we did not assess body composition, Coe et al. (6) reported lower fat and muscle mass in Akita mice, with the loss of fat mass being proportionately larger. Because bone mass is highly correlated with body mass (46), skeletal changes in Akita mice may be less confounded by changes in body weight. In addition, Akita mice have a milder phenotype than similarly hyperglycemic STZ-induced mice (6), and are free from hazards associated with STZ, which is classified as a category 1B carcinogen. Another important advantage of using STZ to induce diabetes is that it can be administered to any strain of mice (or rat), including those that are genetically modified. One limitation in working with Akita mice, is the sex-dependent diabetic phenotype, which precludes direct comparisons between males and females. Finally, a limitation of our study is that we did not include later timepoints to test if the impaired healing seen in Akita mice at 14 and 21 days persists. Thus, we cannot distinguished between delayed healing versus permanently impaired healing.

In summary, young-adult male Akita mice have impaired fracture healing, with smaller cartilage and bone callus size and inferior mechanical properties compared to WT littermates, similar to other T1DM rodent models. In contrast to other models, we find no evidence of accelerated osteoclast resorption of cartilage in Akita mice, and hypothesize that their callus phenotype is due to primary bone and cartilage anabolic deficits. In addition, intact bones of Akita mice have reduced cortical and cancellous bone mass in association with low bone formation. Whole-bone stiffness and strength are also lower in Akita mice, attributed primarily to their smaller size, but with no evidence of embrittlement. We conclude that Akita mice are a useful model to study the biology and treatment of skeletal complications associated with T1DM.

Supplementary Material

Refer to Web version on PubMed Central for supplementary material.

Acknowledgments

Supported by grants from the Orthopedic Research and Education Foundation (OREF) and the NIH/NIAMS (R21 AR066798, R01 AR050211). We thank Mr. Daniel Leib, Ms. Crystal Idleburg and Ms. Samantha Coleman for their assistance with microCT and histology, supported by the Washington University Musculoskeletal Research Center (NIH P30 AR057235 and AR074992, and S10 RR023660). We acknowledge support from the Hope Center Alafi Neuroimaging Lab (NCRR 1S10RR027552) and a Neuroscience Blueprint Interdisciplinary Center Core. We thank the Genome Technology Access Center in the Department of Genetics at Washington University School of Medicine for assistance with qPCR; the Center is partially supported by NCI Cancer Center Support Grant P30 CA91842 to the Siteman Cancer Center, and by ICTS/CTSA Grant# UL1TR002345 from the National Center for Advancing Translational Sciences (NCATS). We thank Core Laboratory for Clinical Studies (CLCS) at Washington University School of Medicine for serum testing.

References

1. Alblowi J, Kayal RA, Siqueira M, McKenzie E, Krothapalli N, McLean J, Conn J, Nikolajczyk B, Einhorn TA, Gerstenfeld L, and Graves DT High levels of tumor necrosis factor-alpha contribute to accelerated loss of cartilage in diabetic fracture healing. Am J Pathol 175:1574–85; 2009. [PubMed: 19745063]
2. Alharbi MA, Zhang C, Lu C, Milovanova TN, Yi L, Ryu JD, Jiao H, Dong G, O'Connor JP, and Graves DT FOXO1 Deletion Reverses the Effect of Diabetic-Induced Impaired Fracture Healing. Diabetes 67:2682–2694; 2018. [PubMed: 30279162]
3. Botolin S, and McCabe LR Bone loss and increased bone adiposity in spontaneous and pharmacologically induced diabetic mice. Endocrinology 148:198–205; 2007. [PubMed: 17053023]
4. Carvalho FR, Calado SM, Silva GA, Diogo GS, Moreira da Silva J, Reis RL, Cancela ML, and Gavaia PJ Altered bone microarchitecture in a type 1 diabetes mouse model Ins2(Akita). J Cell Physiol 234:9338–9350; 2019. [PubMed: 30317631]
5. Chiang JL, Kirkman MS, Laffel LM, Peters AL, and Type 1 Diabetes Sourcebook, A. Type 1 diabetes through the life span: a position statement of the American Diabetes Association. Diabetes Care 37:2034–54; 2014. [PubMed: 24935775]
6. Coe LM, Zhang J, and McCabe LR Both spontaneous Ins2(+/−) and streptozotocin-induced type I diabetes cause bone loss in young mice. J Cell Physiol 228:689–95; 2013. [PubMed: 22886636]
7. Cooke DW, and Plotnick L Type 1 diabetes mellitus in pediatrics. Pediatr Rev 29:374–84; quiz 385; 2008. [PubMed: 18977856]
8. Follak N, Kloting I, and Merk H Influence of diabetic metabolic state on fracture healing in spontaneously diabetic rats. Diabetes Metab Res Rev 21:288–96; 2005. [PubMed: 15693070]
9. Fulzele K, and Clemens TL Novel functions for insulin in bone. Bone 50:452–6; 2012. [PubMed: 21723973]

10. Funk JR, Hale JE, Carmines D, Gooch HL, and Hurwitz SR Biomechanical evaluation of early fracture healing in normal and diabetic rats. J Orthop Res 18:126–32; 2000. [PubMed: 10716288]
11. Gaissmaier C, Koh JL, and Weise K Growth and differentiation factors for cartilage healing and repair. Injury 39 Suppl 1:S88–96; 2008. [PubMed: 18313476]
12. Gandhi A, Beam HA, O'Connor JP, Parsons JR, and Lin SS The effects of local insulin delivery on diabetic fracture healing. Bone 37:482–90; 2005. [PubMed: 16027060]
13. Goldberg VM, Powell A, Shaffer JW, Zika J, Bos GD, and Heiple KG Bone grafting: role of histocompatibility in transplantation. J Orthop Res 3:389–404; 1985. [PubMed: 3906062]
14. Hernandez RK, Do TP, Critchlow CW, Dent RE, and Jick SS Patient-related risk factors for fracture-healing complications in the United Kingdom General Practice Research Database. Acta Orthop 83:653–60; 2012. [PubMed: 23140093]
15. Hygum K, Starup-Linde J, Harslof T, Vestergaard P, and Langdahl BL MECHANISMS IN ENDOCRINOLOGY: Diabetes mellitus, a state of low bone turnover - a systematic review and meta-analysis. Eur J Endocrinol 176:R137–R157; 2017. [PubMed: 28049653]
16. Iitsuka N, Hie M, and Tsukamoto I Zinc supplementation inhibits the increase in osteoclastogenesis and decrease in osteoblastogenesis in streptozotocin-induced diabetic rats. Eur J Pharmacol 714:41–7; 2013. [PubMed: 23735664]
17. Janghorbani M, Feskanich D, Willett WC, and Hu F Prospective study of diabetes and risk of hip fracture: the Nurses' Health Study. Diabetes Care 29:1573–8; 2006. [PubMed: 16801581]
18. Janghorbani M, Van Dam RM, Willett WC, and Hu FB Systematic review of type 1 and type 2 diabetes mellitus and risk of fracture. Am J Epidemiol 166:495–505; 2007. [PubMed: 17575306]
19. Jepsen KJ, Silva MJ, Vashishth D, Guo XE, and van der Meulen MC Establishing biomechanical mechanisms in mouse models: practical guidelines for systematically evaluating phenotypic changes in the diaphyses of long bones. J Bone Miner Res 30:951–66; 2015. [PubMed: 25917136]
20. Jiao H, Xiao E, and Graves DT Diabetes and Its Effect on Bone and Fracture Healing. Curr Osteoporos Rep 13:327–35; 2015. [PubMed: 26254939]
21. Kayal RA, Alblowi J, McKenzie E, Krothapalli N, Silkman L, Gerstenfeld L, Einhorn TA, and Graves DT Diabetes causes the accelerated loss of cartilage during fracture repair which is reversed by insulin treatment. Bone 44:357–63; 2009. [PubMed: 19010456]
22. Kayal RA, Siqueira M, Alblowi J, McLean J, Krothapalli N, Faibish D, Einhorn TA, Gerstenfeld LC, and Graves DT TNF-alpha mediates diabetes-enhanced chondrocyte apoptosis during fracture healing and stimulates chondrocyte apoptosis through FOXO1. J Bone Miner Res 25:1604–15; 2010. [PubMed: 20200974]
23. Kayal RA, Tsatsas D, Bauer MA, Allen B, Al-Sebaei MO, Kakar S, Leone CW, Morgan EF, Gerstenfeld LC, Einhorn TA, and Graves DT Diminished bone formation during diabetic fracture healing is related to the premature resorption of cartilage associated with increased osteoclast activity. J Bone Miner Res 22:560–8; 2007. [PubMed: 17243865]
24. Kayo T, and Koizumi A Mapping of murine diabetogenic gene mody on chromosome 7 at D7Mit258 and its involvement in pancreatic islet and beta cell development during the perinatal period. J Clin Invest 101:2112–8; 1998. [PubMed: 9593767]
25. Kitabchi AE, Umpierrez GE, Miles JM, and Fisher JN Hyperglycemic crises in adult patients with diabetes. Diabetes Care 32:1335–43; 2009. [PubMed: 19564476]
26. Lim JC, Ko KI, Mattos M, Fang M, Zhang C, Feinberg D, Sindi H, Li S, Alblowi J, Kayal RA, Einhorn TA, Gerstenfeld LC, and Graves DT TNFalpha contributes to diabetes impaired angiogenesis in fracture healing. Bone 99:26–38; 2017. [PubMed: 28285015]
27. Liu X, McKenzie JA, Maschhoff CW, Gardner MJ, and Silva MJ Exogenous hedgehog antagonist delays but does not prevent fracture healing in young mice. Bone 103:241–251; 2017. [PubMed: 28734986]
28. Lu Y, Alharbi M, Zhang C, O'Connor JP, and Graves DT Deletion of FOXO1 in chondrocytes rescues the effect of diabetes on mechanical strength in fracture healing. Bone 123:159–167; 2019. [PubMed: 30904630]
29. Martin LM, and McCabe LR Type I diabetic bone phenotype is location but not gender dependent. Histochem Cell Biol 128:125–33; 2007. [PubMed: 17609971]

30. McCabe LR Understanding the pathology and mechanisms of type I diabetic bone loss. J Cell Biochem 102:1343–57; 2007. [PubMed: 17975793]

31. McKenzie JA, Maschhoff C, Liu X, Migotsky N, Silva MJ, and Gardner MJ Activation of hedgehog signaling by systemic agonist improves fracture healing in aged mice. J Orthop Res 37:51–59; 2019. [PubMed: 29663560]

32. Motyl K, and McCabe LR Streptozotocin, type I diabetes severity and bone. Biol Proced Online 11:296–315; 2009. [PubMed: 19495918]

33. Moyer-Mileur LJ, Slater H, Jordan KC, and Murray MA IGF-1 and IGF-binding proteins and bone mass, geometry, and strength: relation to metabolic control in adolescent girls with type 1 diabetes. J Bone Miner Res 23:1884–91; 2008. [PubMed: 18665784]

34. Nyman JS, Even JL, Jo CH, Herbert EG, Murry MR, Cockrell GE, Wahl EC, Bunn RC, Lumpkin CK Jr., Fowlkes JL, and Thrailkill KM Increasing duration of type 1 diabetes perturbs the strength-structure relationship and increases brittleness of bone. Bone 48:733–40; 2011. [PubMed: 21185416]

35. Ogasawara A, Nakajima A, Nakajima F, Goto K, and Yamazaki M Molecular basis for affected cartilage formation and bone union in fracture healing of the streptozotocin-induced diabetic rat. Bone 43:832–9; 2008. [PubMed: 18725334]

36. Ohuchi K, Miyakoshi N, Kasukawa Y, Segawa T, Kinoshita H, Sato C, Fujii M, and Shimada Y Effects of teriparatide on bone in autochthonous transgenic model mice for diabetes mellitus (Akita mice). Osteoporos Sarcopenia 5:109–115; 2019. [PubMed: 31938729]

37. Oyadomari S, Koizumi A, Takeda K, Gotoh T, Akira S, Araki E, and Mori M Targeted disruption of the Chop gene delays endoplasmic reticulum stress-mediated diabetes. J Clin Invest 109:525–32; 2002. [PubMed: 11854325]

38. Parajuli A, Liu C, Li W, Gu X, Lai X, Pei S, Price C, You L, Lu XL, and Wang L Bone's responses to mechanical loading are impaired in type 1 diabetes. Bone 81:152–160; 2015. [PubMed: 26183251]

39. Ron D Proteotoxicity in the endoplasmic reticulum: lessons from the Akita diabetic mouse. J Clin Invest 109:443–5; 2002. [PubMed: 11854314]

40. Rosa SC, Rufino AT, Judas F, Tenreiro C, Lopes MC, and Mendes AF Expression and function of the insulin receptor in normal and osteoarthritic human chondrocytes: modulation of anabolic gene expression, glucose transport and GLUT-1 content by insulin. Osteoarthritis Cartilage 19:719–27; 2011. [PubMed: 21324373]

41. Rossini AA, Like AA, Chick WL, Appel MC, and Cahill GF Jr. Studies of streptozotocin-induced insulitis and diabetes. Proc Natl Acad Sci U S A 74:2485–9; 1977. [PubMed: 142253]

42. Rother KI Diabetes treatment--bridging the divide. N Engl J Med 356:1499–501; 2007. [PubMed: 17429082]

43. Saito M, Fujii K, Mori Y, and Marumo K Role of collagen enzymatic and glycation induced cross-links as a determinant of bone quality in spontaneously diabetic WBN/Kob rats. Osteoporos Int 17:1514–23; 2006. [PubMed: 16770520]

44. Shi Y, and Hu FB The global implications of diabetes and cancer. Lancet 383:1947–8; 2014. [PubMed: 24910221]

45. Silva MJ, Brodt MD, Lynch MA, McKenzie JA, Tanouye KM, Nyman JS, and Wang X Type 1 diabetes in young rats leads to progressive trabecular bone loss, cessation of cortical bone growth, and diminished whole bone strength and fatigue life. J Bone Miner Res 24:1618–27; 2009. [PubMed: 19338453]

46. Silva MJ, Eekhoff JD, Patel T, Kenney-Hunt JP, Brodt MD, Steger-May K, Scheller EL, and Cheverud JM Effects of High-Fat Diet and Body Mass on Bone Morphology and Mechanical Properties in 1100 Advanced Intercross Mice. J Bone Miner Res 34:711–725; 2019. [PubMed: 30615803]

47. Verhaeghe J, Suiker AM, Visser WJ, Van Herck E, Van Bree R, and Bouillon R The effects of systemic insulin, insulin-like growth factor-I and growth hormone on bone growth and turnover in spontaneously diabetic BB rats. J Endocrinol 134:485–92; 1992. [PubMed: 1402554]

48. Vestergaard P Discrepancies in bone mineral density and fracture risk in patients with type 1 and type 2 diabetes--a meta-analysis. Osteoporos Int 18:427–44; 2007. [PubMed: 17068657]

49. Wang J, Takeuchi T, Tanaka S, Kubo SK, Kayo T, Lu D, Takata K, Koizumi A, and Izumi T A mutation in the insulin 2 gene induces diabetes with severe pancreatic beta-cell dysfunction in the Mody mouse. J Clin Invest 103:27–37; 1999. [PubMed: 9884331]

50. Wang Z, and Gleichmann H GLUT2 in pancreatic islets: crucial target molecule in diabetes induced with multiple low doses of streptozotocin in mice. Diabetes 47:50–6; 1998. [PubMed: 9421374]

51. Weiss RE, and Reddi AH Influence of experimental diabetes and insulin on matrix-induced cartilage and bone differentiation. Am J Physiol 238:E200–7; 1980. [PubMed: 6989262]

52. White CB, Turner NS, Lee GC, and Haidukewych GJ Open ankle fractures in patients with diabetes mellitus. Clin Orthop Relat Res:37–44; 2003.

53. Yoshioka M, Kayo T, Ikeda T, and Koizumi A A novel locus, Mody4, distal to D7Mit189 on chromosome 7 determines early-onset NIDDM in nonobese C57BL/6 (Akita) mutant mice. Diabetes 46:887–94; 1997. [PubMed: 9133560]

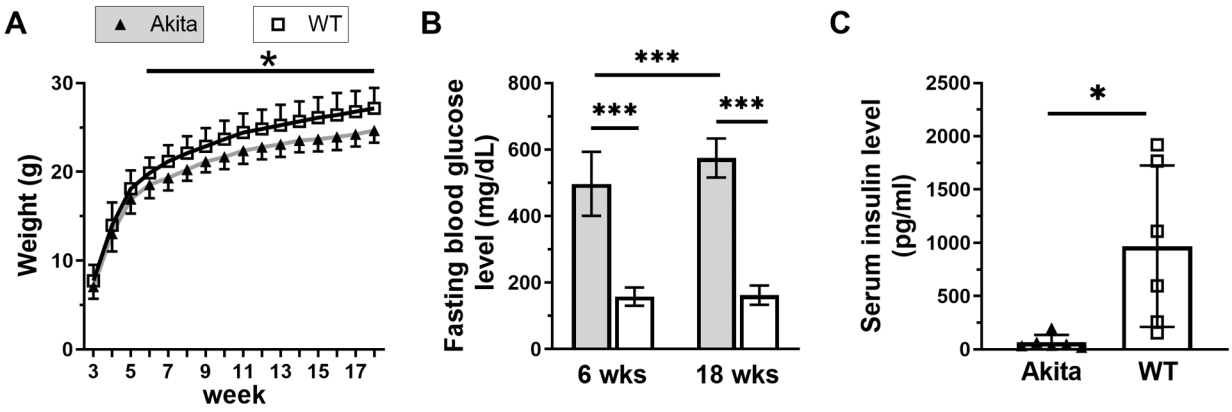

Figure 1. Male Akita mice are hyperglycemic and hypoinsulinemic.

A) Akita and WT mice had similar initial body weights and both gained weight from 3 to 18 weeks, although Akita mice had 6–9% lower body weight after 6 weeks age (n = 28–40). B) Fasting blood glucose levels indicated that all Akita mice were hyperglycemic by 6 weeks with increased severity at 18 weeks (n = 69–98). C) At 18 weeks Akita mice had a severe insulin deficiency (n = 6). (*p <0.05, ***p<0.001, Akita vs. WT)

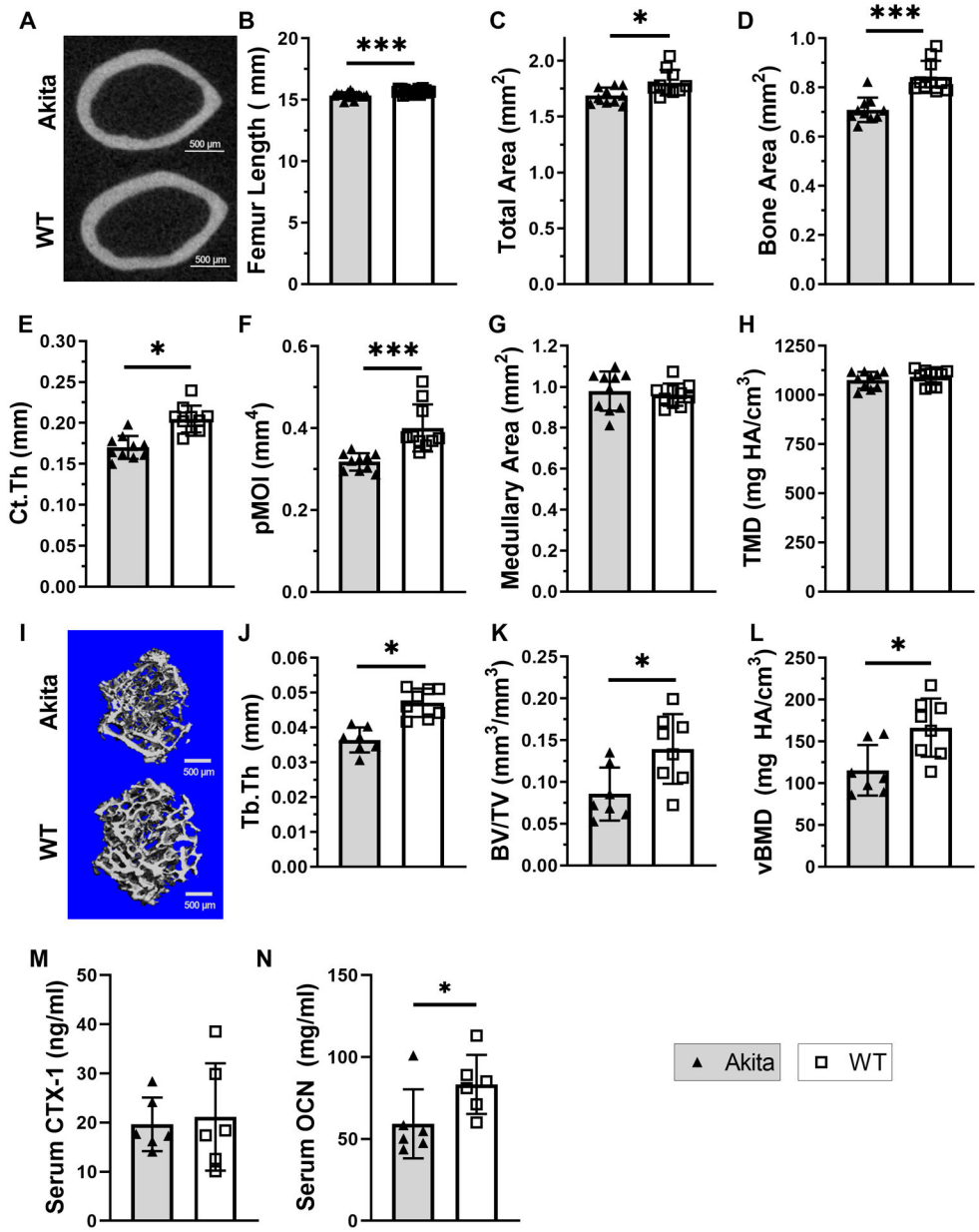

Figure 2. Akita mice are osteopenic at 21 weeks of age.

A) Representative microCT sections of Akita and WT intact femur cortical bone. B) Akita mice had a slightly shorter femur than WT. C-H) Cortical bone microCT evaluation (n = 8–11) revealed that Akita femurs had reduced total area, bone area, Ct.Th and pMOI compared to WT, while medullary area and TMD were not different between groups. I) Representative 3D reconstruction of Akita and WT cancellous bone from intact distal femur. J-L) Cancellous bone microCT evaluation (n = 7–8) revealed that Akita femurs had reduced trabecular thickness, BV/TV and volumetric BMD. M-N) Serum analysis of bone turnover markers CTX-1 (resorption) and OCN (formation) (n=6). (*p<0.05, ***p<0.001, Akita vs. WT)

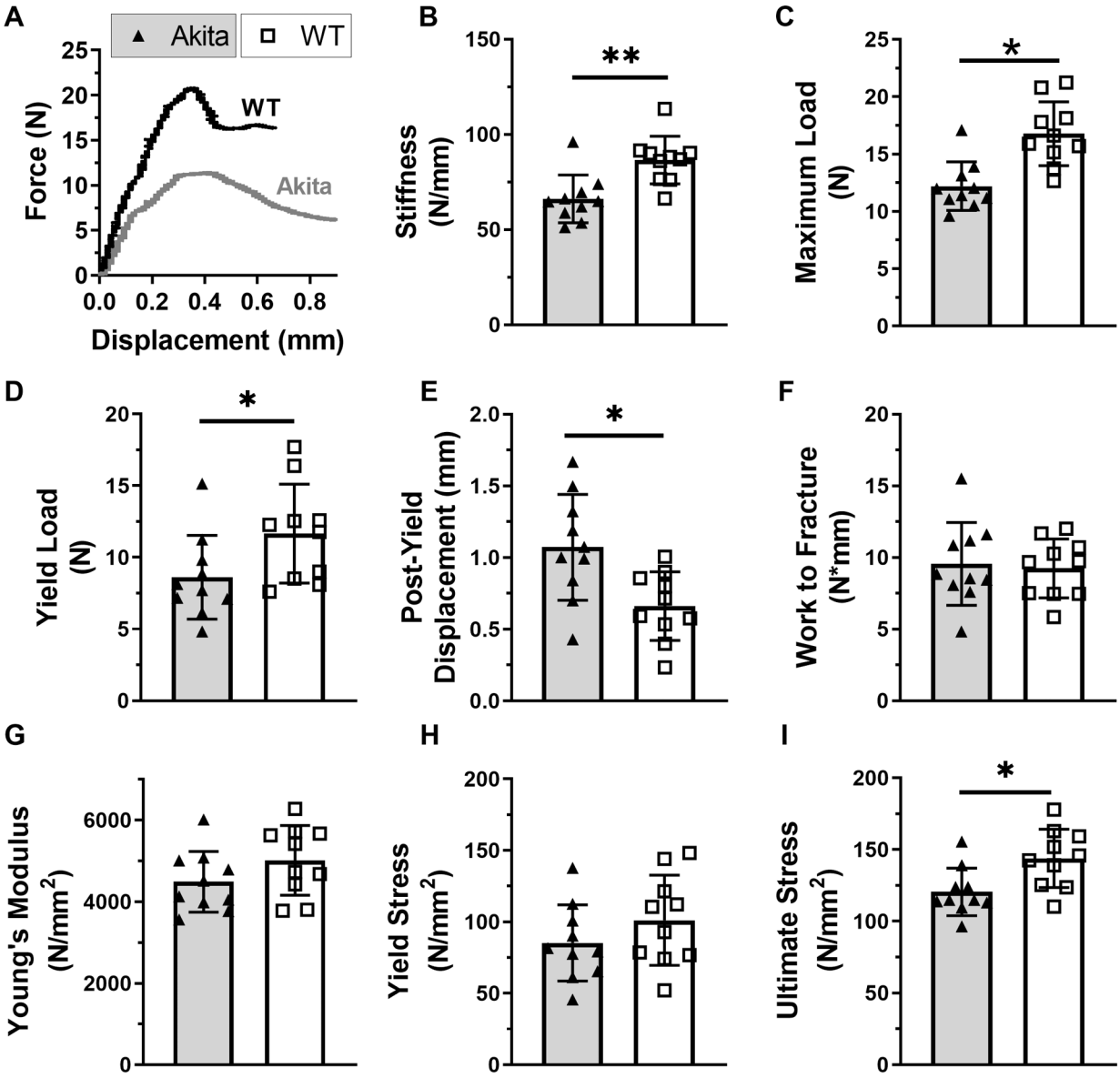

Figure 3. Whole-bone strength is diminished in Akita bones at 21 weeks.

A) Representative three-point bending force-displacement curves for Akita and WT femurs. B-F) Structural property evaluation (n = 10) revealed that Akita femurs had decreased stiffness, maximum load, and yield load, with increased post-yield displacement. There were no differences in work to fracture. G-I) Material properties calculations of Young's modulus and yield stress were not different, while ultimate stress was decreased in Akita femurs. (*p<0.05, **p<0.01, Akita vs. WT)

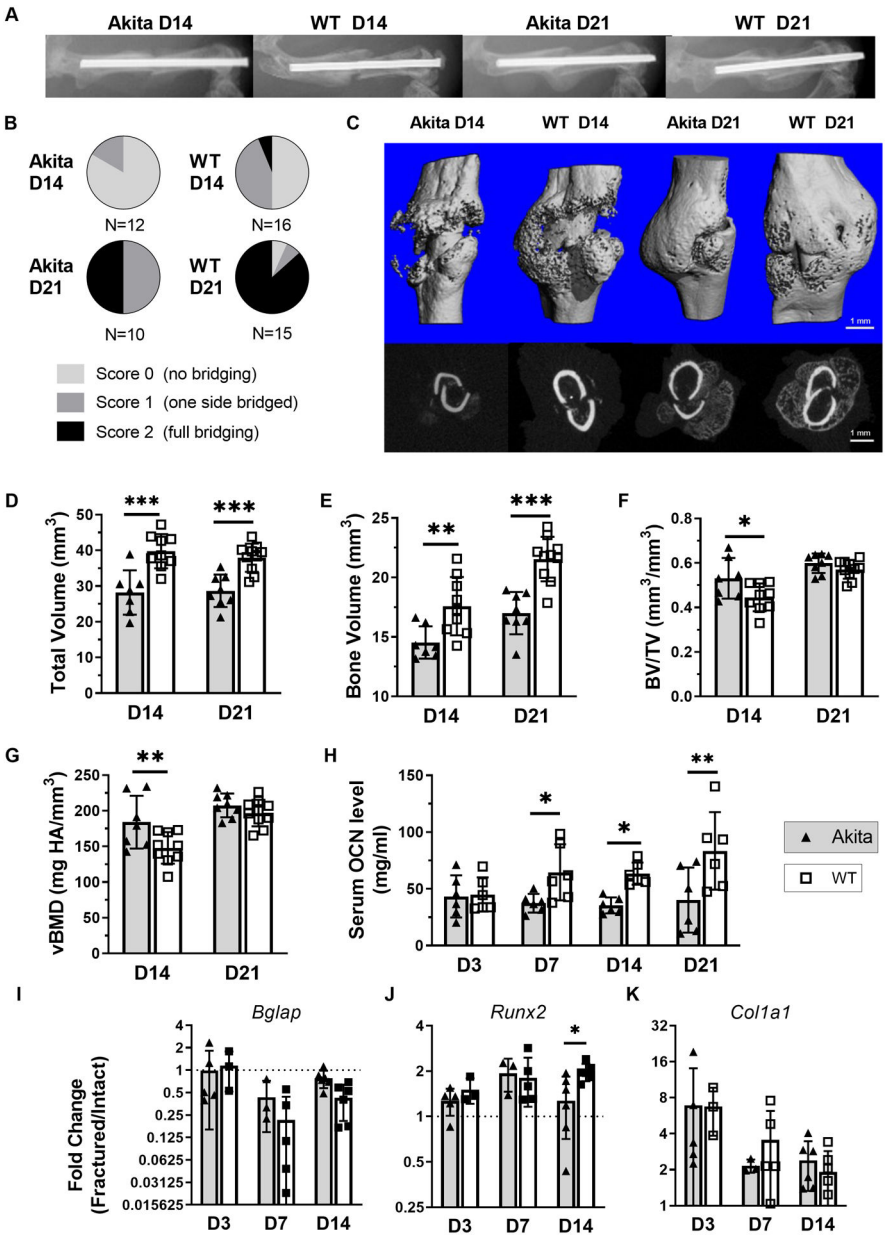

Figure 4. Akita mice had diminished bone formation following fracture.

A) Representative x-ray images at days 14 and 21 after fracture. B) Quantification of x-ray images found significantly less union rates at day 21 ($p < 0.05$ Chi-squared test). C) Representative microCT reconstructions of day 14 and 21 post fracture (6.3mm, 300 slices) and two-dimensional cross sections at the callus midpoint. (These are from the same samples shown in A.) D-G) At day 14 Akita calluses had a significantly lower total volume and bone volume, with significantly higher BV/TV and vBMD (n = 7–9). At day 21 Akita calluses had lower total volume and bone volume, while BV/TV and vBMD were no different (n = 8–10). H) Akita mice had reduced serum OCN levels at day 7, day 14 and day 21 groups (n = 6). I-K) Expression of osteogenic genes was similar on days 3, 7 and

14 between groups, with the exception of *Runx2* being lower in Akita at day 14 (n = 3–6). (*p<0.05, **p<0.01, ***p<0.001, Akita vs. WT)

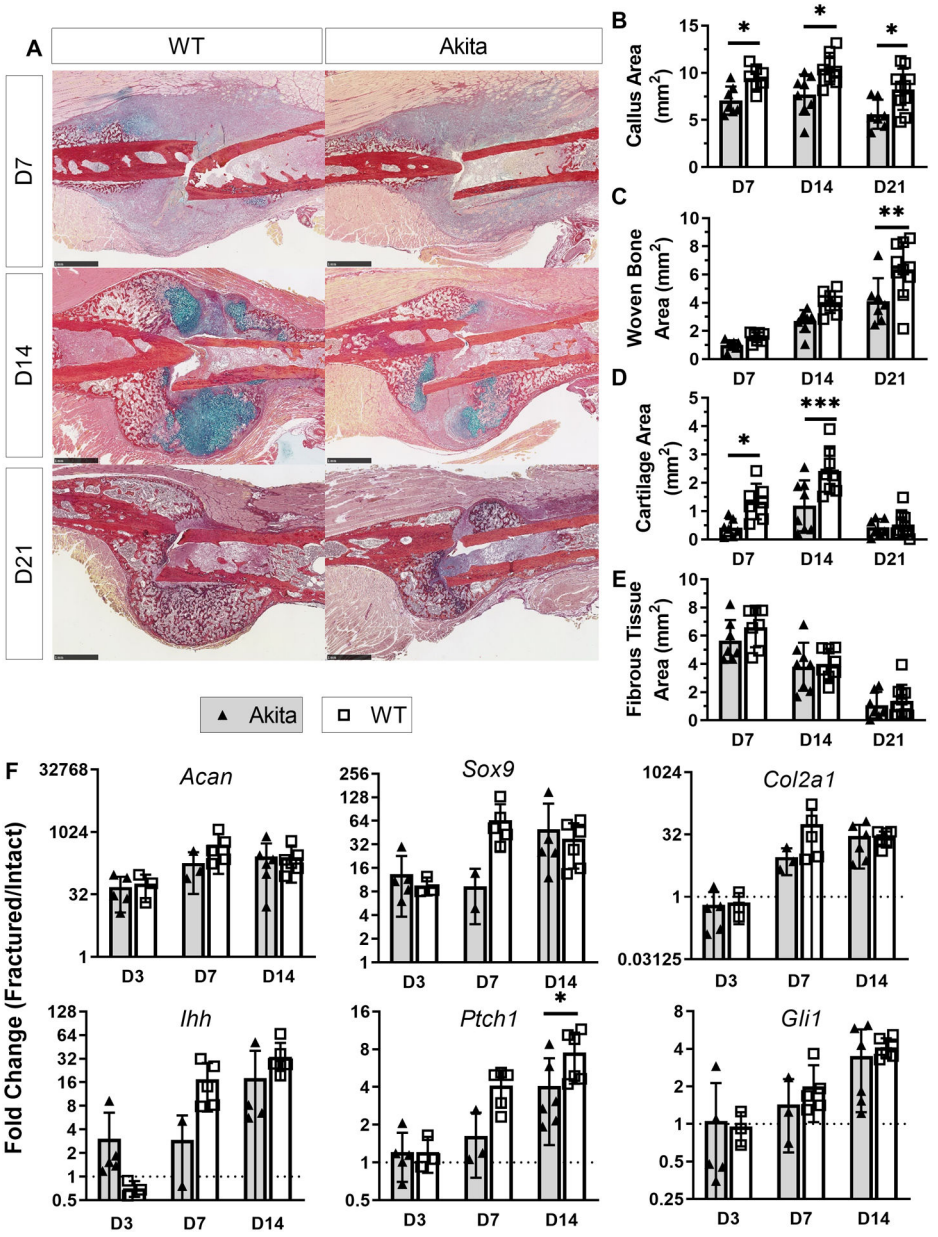

Figure 5. Akita mice had impaired cartilage formation after fracture.

A) Representative picrosirius red/Alcian blue staining at days 7, 14 and 21. B-E) Analysis of staining revealed Akita mice had decreased callus area at all time points with decreased woven bone area on day 21, and cartilage area on days 7 and 14 (n = 7–11). F) The expression of chondrogenic genes (*Acan*, *Sox9* and *Col2a1*) substantially increased after fracture in both Akita and WT. Expression of hedgehog pathway related genes (*Ihh*, *Ptch1* and *Gli1*) was increased in both groups over time (n = 3–6). (*p<0.05, **p<0.01, ***p<0.001, Akita vs. WT; scale bar 1 mm)

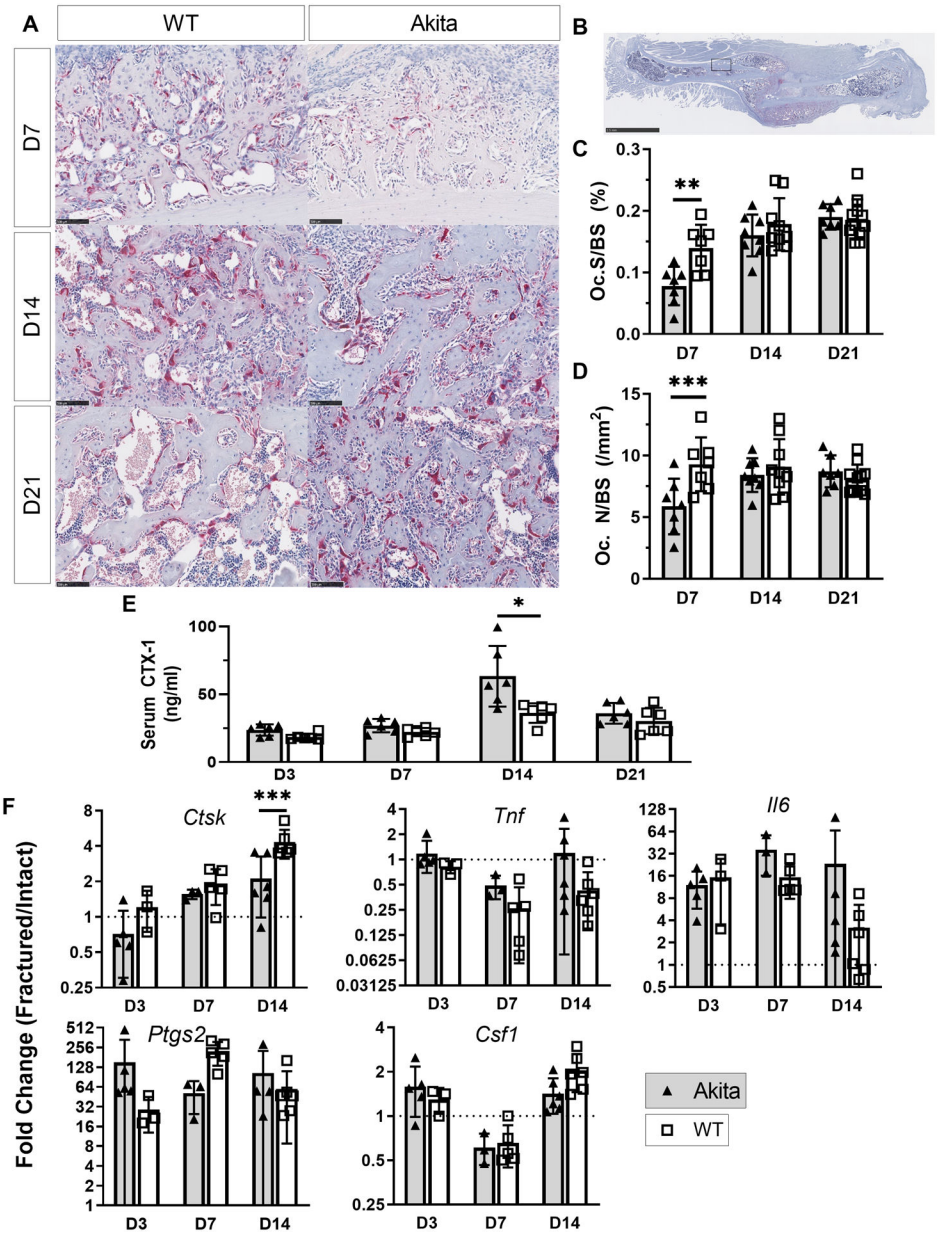

Figure 6. Osteoclasts were modestly affected in Akita mice.

A-B) Representative tartrate-resistant acid phosphatase (TRAP) staining at days 7, 14 and 21 post fracture. C-D) Histological analysis revealed Oc.S/BS and Oc.N/BS were decreased in Akita mice on day 7 (n = 7–11). E) Elevated serum CTX-1 levels were observed at day 14 for Akita mice (n = 6). F) Expression of osteoclastogenic and inflammatory genes at days 3, 7 and 14 were not different between groups, with the exception of *Ctsk* at day 14 (n = 3–6). (*p<0.05, **p<0.01, ***p<0.001, Akita vs. WT; scale bar A: 100 μm, B: 2.5 mm)

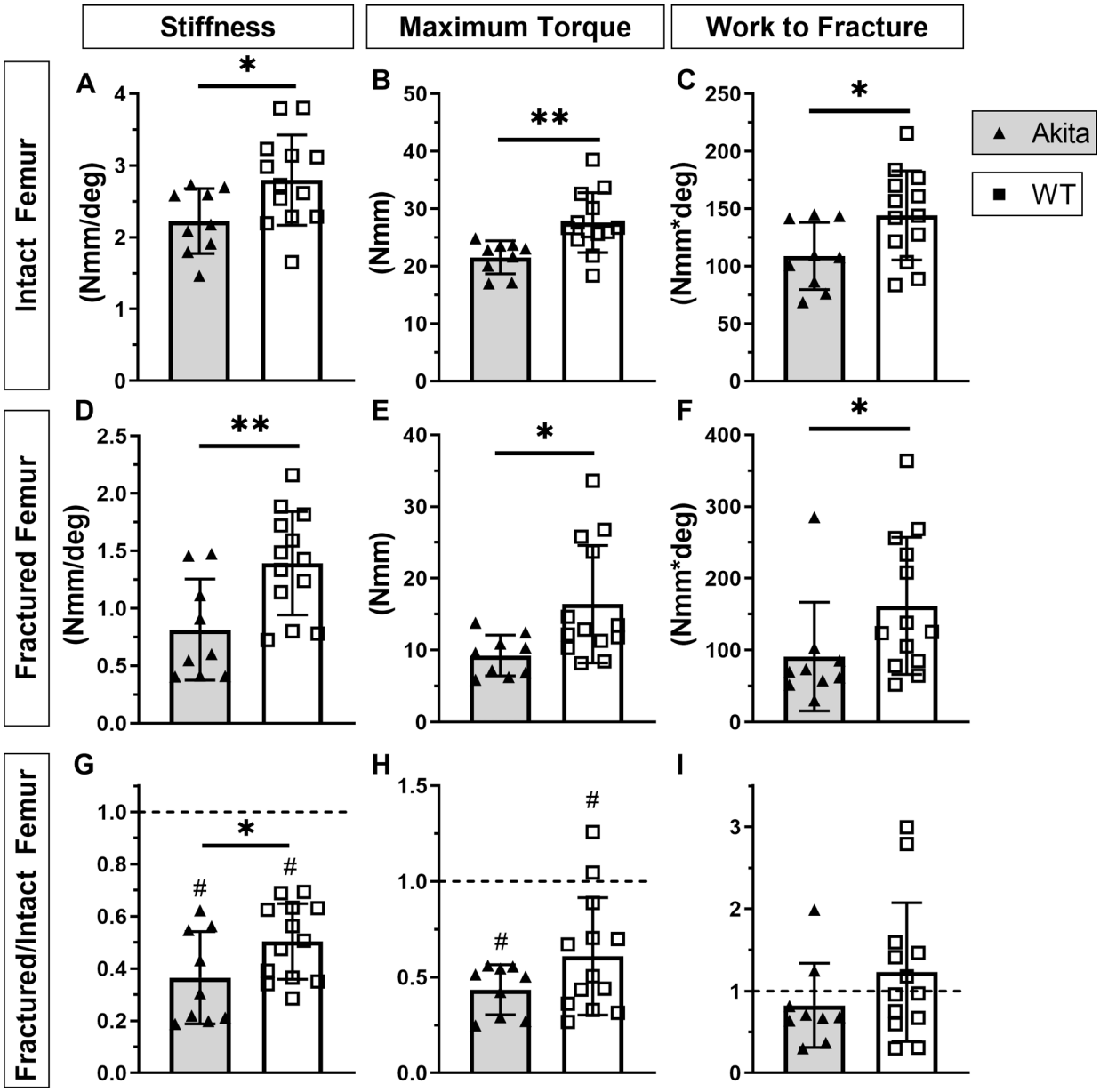

Figure 7. Akita fracture callus is mechanically inferior.

A-C) Intact Akita femurs had decreased stiffness, maximum torque and work to fracture (n = 10). D-F) At day 21 post fracture healing Akita femurs (fracture callus) had decreased stiffness, maximum torque and work to fracture compared to WT. G-I) Normalized data (fractured/intact) revealed that stiffness and maximum torque for both groups were reduced in fracture compared to intact femur, with a significant decrease in stiffness for Akita compared to WT. Work to fracture recovered to intact levels in both groups. (*p<0.05, **p<0.01, Akita vs. WT; #p<0.01, fracture vs. intact)